Coupling optimized bending-insensitive multi-core fibers for lensless endoscopy

Naveen Gajendra Kumar, Siddharth Sivankutty, Victor Tsvirkun, Andy Cassez, Damien Labat, Rosa Cossart, Geraud Bouwmans, Esben Ravn Andresen, Hervé Rigneault

Research Article | Vol. 31, No. 10 / 8 May 2023 / Optics Express 15334
Optics EXPRESS

Coupling optimized bending-insensitive multi-core fibers for lensless endoscopy

NAVEEN GAJENDRA KUMAR,[1] SIDDHARTH SIVANKUTTY,[2] VICTOR TSVIRKUN,[1] ANDY CASSEZ,[2] DAMIEN LABAT,[2] ROSA COSSART,[3] GERAUD BOUWMANS,[2] ESBEN RAVN ANDRESEN,[2,4] AND HERVÉ RIGNEAULT[1,*]

[1]*Aix Marseille Univ, CNRS, Institut Fresnel, Turing Centre for Living systems, Marseille, France*
[2]*University of Lille, CNRS, UMR 8523, PhLAM-Physique des Lasers Atomes et Molécules, Lille, France*
[3]*Aix Marseille Univ, Inserm, INMED, Turing Center for Living Systems, Marseille, France*
[4]*esben.andresen@ircica.univ-lille1.fr*
[*]*herve.rigneault@fresnel.fr*

Abstract: We report a bending-insensitive multi-core fiber (MCF) for lensless endoscopy imaging with modified fiber geometry that enables optimal light coupling in and out of the individual cores. In a previously reported bending insensitive MCF (twisted MCF), the cores are twisted along the length of the MCF allowing for the development of flexible thin imaging endoscopes with potential applications in dynamic and freely moving experiments. However, for such twisted MCFs the cores are seen to have an optimum coupling angle which is proportional to their radial distance from the center of the MCF. This brings coupling complexity and potentially degrades the endoscope imaging capabilities. In this study, we demonstrate that by introducing a small section (1 cm) at two ends of the MCF, where all the cores are straight and parallel to the optical axis one can rectify the above coupling and output light issues of the twisted MCF, enabling the development of bend-insensitive lensless endoscopes.

1. Introduction

One of the main challenges of in-vivo optical deep tissue imaging is the scattering of ballistic photons by tissues which limits the penetration depth of conventional imaging techniques. Nonlinear multiphoton imaging techniques can partially circumvent this problem as NIR wavelengths are less scattered and thus can penetrate deeper into the tissue. However, even here the penetration depth is still limited to 1 mm [1]. One way to overcome this limitation is to miniaturize the imaging system to such an extent that it can be inserted into the tissue in a minimally invasive way in order to reach the desired imaging plane. "Lensless" endoscopy based on multimode [2] or multi-core fibers (MCFs) with single-mode cores [3] is one such technique. Here, a thin and flexible optical fiber is used to deliver the excitation light to the image plane and collect the back-scattered fluorescence signal without the need for any distal optics. Lensless endoscopy is possible through measurement of the transmission matrix of the optical fiber [4] and using this knowledge to manipulate the phase of the field injected into the waveguide using a device like a 2D spatial light modulator (SLM). The distal head of such an endoscope is as thin as the optical fiber itself and when combined with 2-photon fluorescence (2PEF) imaging [5–7] it opens the road to develop a powerful tool for minimally invasive deep tissue imaging. In MCF-based lensless endoscopes [8,9], the optical fibers are designed to have large core pitch distances. Due to the large spacing between neighbouring cores there is very little mode coupling between them leading to a diagonal transmission matrix. Thus the phase of the exit field for a given core only depends on the phase of the input field for that core. Once the transmission matrix of the MCF is measured, this allows for full control of the phase of the fields at the distal end of the fiber by controlling the phase at the proximal end [9–12].

#485550 https://doi.org/10.1364/OE.485550
Journal © 2023 Received 16 Jan 2023; revised 6 Mar 2023; accepted 20 Mar 2023; published 24 Apr 2023

Optics EXPRESS

2PEF imaging experiments using lensless miniature endoscopes are appealing for neurobiologists because they allow the imaging of the deep brain neuron network activity [13,14], potentially on freely moving mice that could interact with other animals. Freely moving experiments provide valuable data about cranial functions that are inherently dependent on the test animal's spatial environment. In the scope of such freely moving 2PEF imaging experiments, one expects the flexible endoscope to bend and these conformational changes would modify the fiber transmission matrix [15], possibly precluding imaging. Such geometrical contributions should be avoided entirely or corrected in real-time in order to gain full functionality of the endoscope. We have shown that this fundamental problem can be circumvented with the use of twisted MCFs which are designed to have a transfer matrix independent of bending of the endoscope [16]. Such twisted MCFs have cores twisted along their length with a helical period P as shown in Fig. 1. For the twisted MCF to be bend insensitive, the length of the twisted MCF L must be an integer multiple of the twist period P, and P must be sufficiently smaller than the radius of curvature of the bending [16].

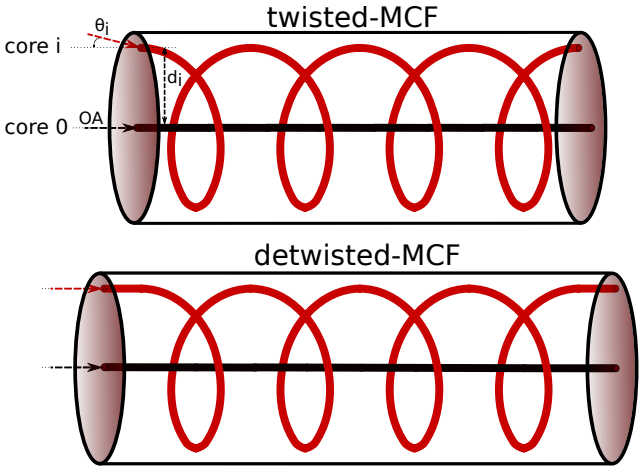

Fig. 1. Coupling into a (top) twisted MCF and a (bottom) detwisted MCF. In the twisted MCF θ^i is proportional to the radial distance of the core from the center of the MCF whereas $\theta^i = 0$ in a straight or detwisted MCF

However due to the geometry of the twisted MCF, for a given core i, there is a mode mismatch between the Gaussian beam profiles of the input field and the MCF modes. Therefore the input field to each core has to be coupled at an angle θ_x^i and θ_y^i w.r.t the x-axis and y-axis. The value of these angles is proportional to the radial distance d^i of the core from the center of the MCF.

$$\begin{aligned} \sin(\theta_x^i) &= n_{\text{eff}} \frac{2\pi x^i}{P} \\ \sin(\theta_y^i) &= n_{\text{eff}} \frac{2\pi y^i}{P} \end{aligned} \tag{1}$$

Here x^i and y^i are displacements of core i in the x and y direction from the center of the MCF. Figure 2(a) shows the coupling angles across the MCF cores in the case of an aperiodic Fermat MCF core layout that have been shown to extend the field of view of lensless endoscopes [17]. Similarly, at the endoscope MCF distal output, the individual fields from the different cores diverge away from the optical axis resulting in lesser overlap of the fields at the distal planes. For core i the exit field has a propagation vector that can be represented as $\vec{k}^i = k_x^i.\hat{x} + k_y^i.\hat{y} + k_z^i.\hat{z}$. $\theta_x^i = \sin^{-1}(k_x^i/k^i)$ and $\theta_y^i = \sin^{-1}(k_y^i/k^i)$ are the angles $\vec{k}^i$ makes with the x and y axis respectively.

Optics EXPRESS

For MCF-based endoscopes the focal spot at the imaging plane is formed due to the coherent combining of exit fields at the defined imaging plane, the lesser the overlap of the fields at the imaging plane, the lesser the relative power at the focal spot. Due to the sparse spacing of the cores in the MCFs used in lensless endoscopy, the relative power at the focal spot is very small. For a 120-core MCF with cores arranged in a fermat spiral pattern the relative power at the focal spot was numerically found to be 3.45 % of the total power at the focal plane (500 μm from the distal MCF face) and for its twisted counterpart, this value was numerically calculated to be 3.15 %, this decrease in focal intensity is observed in Fig. 2(b) where the normalized focal intensities of a standard MCF is compared to a twisted one. For nonlinear contrast imaging schemes such as 2PEF an intense focal spot is needed in order to induce multiphoton excitation. In [18] it was shown that by functionalizing the distal tip of the MCF with a hyper-telescope micro-structure it is possible to improve the value of relative power at the focal spot to 25 % of the total exit power. However, such a functionalization requires the mode coupled out of each of the cores to be parallel to the optical axis. Therefore there is a need to modify the design of the twisted MCF, to match the coupling in and out of the twisted MCF to that of a normal (straight) MCF, i.e. with $\theta_x = \theta_y = 0$ for the input and output light.

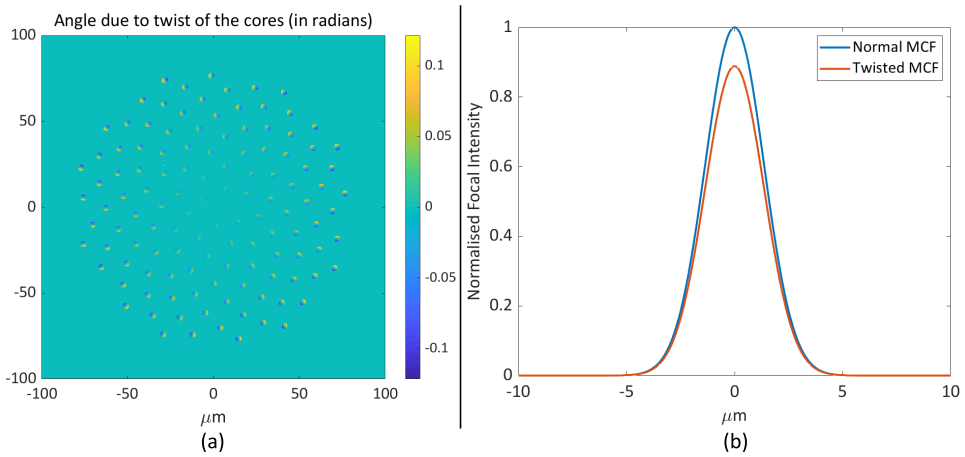

Fig. 2. (a) Numerical representation of coupling angles into different cores of a 120-core twisted Fermat layout MCF [17] with $\Lambda_{mean} = 11.8\,\mu m$ and core MFD = $3.6\,\mu m$. (b) Normalized focal intensity for a normal MCF with straight cores and an MCF with twisted cores (P = 8 mm).

In this letter, we introduce a modified twisted MCF, where 1 cm long sections at the two ends of the fiber are "detwisted" so that all the cores in this section are straight and slowly transitioned into twisted cores as shown in the lower part of Fig. 1. The length of the detwist was heuristically chosen in order to have sections which are small enough that they can be kept static during an imaging experiment. We investigate how this modification helps in optimizing the in- and out-coupling from twisted MCFs without affecting its bending-insensitive transmission matrix. For convenience, these modified twisted MCFs having detwisted sections at their extremities will be referred to as "detwist-MCFs".

2. Experiment and results

The fabrication and characterization of twisted MCFs are described in detail in [16]. The addition of the two small sections (1 cm) at the ends of the twisted MCFs is done by heating the ends with a CO_2 laser-based glass processing and splicing system (LZM-100 Fujikura) and rotating the MCF in the opposite direction of the twists, thus "detwisting" the end of the MCF. The

Optics EXPRESS

desired length of straight MCF is attained by closely controlling the length of fiber heated and the rotation velocity at which the MCF is detwisted. Two different detwisted MCFs were fabricated and tested (30 cm long twist MCF with a 1 cm detwist section), one with a periodic arrangement of cores with a core-to-core distance (Λ) = 16 μm (inset Fig. 3(a)) and one with a Fermat arrangement of cores [17] with an average (Λ) = 11.8 μm (inset Fig. 4(a)). For all MCFs, the diameter of individual cores equals 3.6 μm, and the cores have a parabolic index profile with an index difference relative to the cladding $\Delta n = 30 \cdot 10^{-3}$. Both of the periodic and Fermat MCF (referred to as periodic-detwist-MCF and Fermat-detwist-MCF) are twisted with a helical period of P = 8 mm. The periodic detwist-MCF was used for comparing the coupling angle optimization with its twisted counterparts and the Fermat-detwist-MCF was used to study the sensitivity of the transmission matrix to bending.

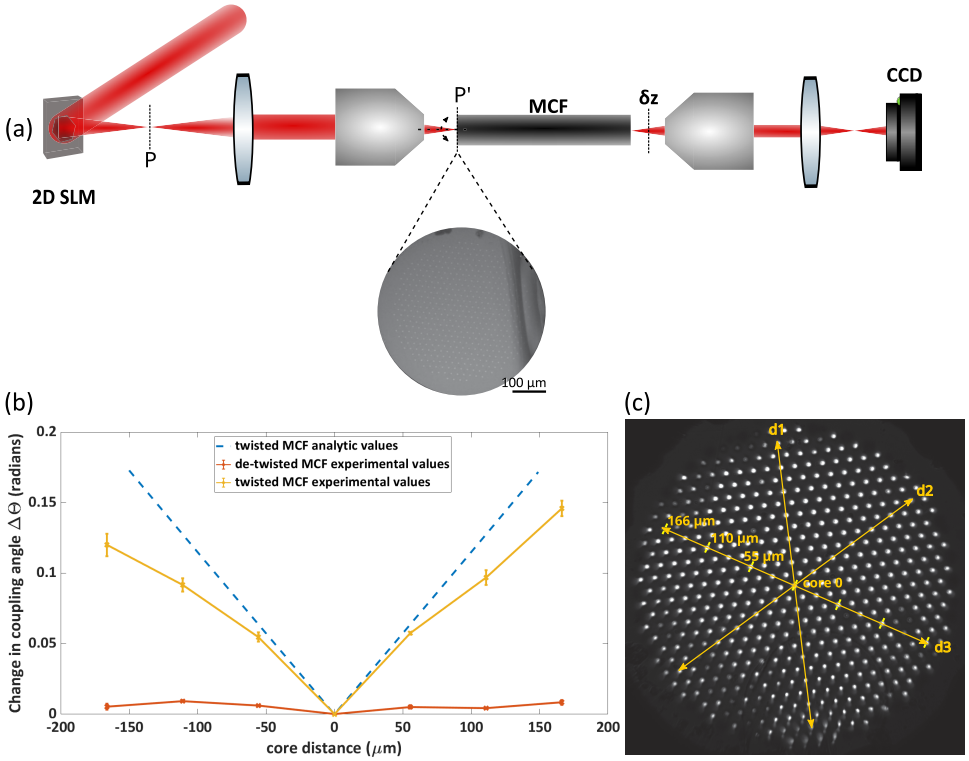

Fig. 3. (a) Setup for coupling angle measurements. Inset shows the SEM image of an MCF with a periodic core distribution. (b) Coupling angle w.r.t radial distance of the core from the MCF axis. (c) Diagonals along which the measurements were taken.

The schematic of the setup used for coupling angle measurements is shown in Fig. 3(a). A continuous wave Yb fiber laser (IPG Laser, GmbH) with λ = 1050 nm was used as the light source. A liquid crystal 2D spatial light modulator (2D SLM, X10468, Hamamatsu) was used to control the phase of the field coupled into the MCF cores. For coupling into a MCF with N cores, a lenslet array with N segments is inscribed on the 2D SLM and then the focal plane of the SLM is imaged onto the MCF distal end with an appropriate de-magnification. The focal plane of the SLM is re-imaged onto P' (the MCF in-coupling plane), thus each of the segments on the SLM is matched to a corresponding core of the MCF. In order to measure the optimal coupling angles for the twisted (and the de-twisted) fibers, we initially perform a calibration to account for the system aberrations. For the measurement, only the central segment of SLM, aligned to the

Optics EXPRESS

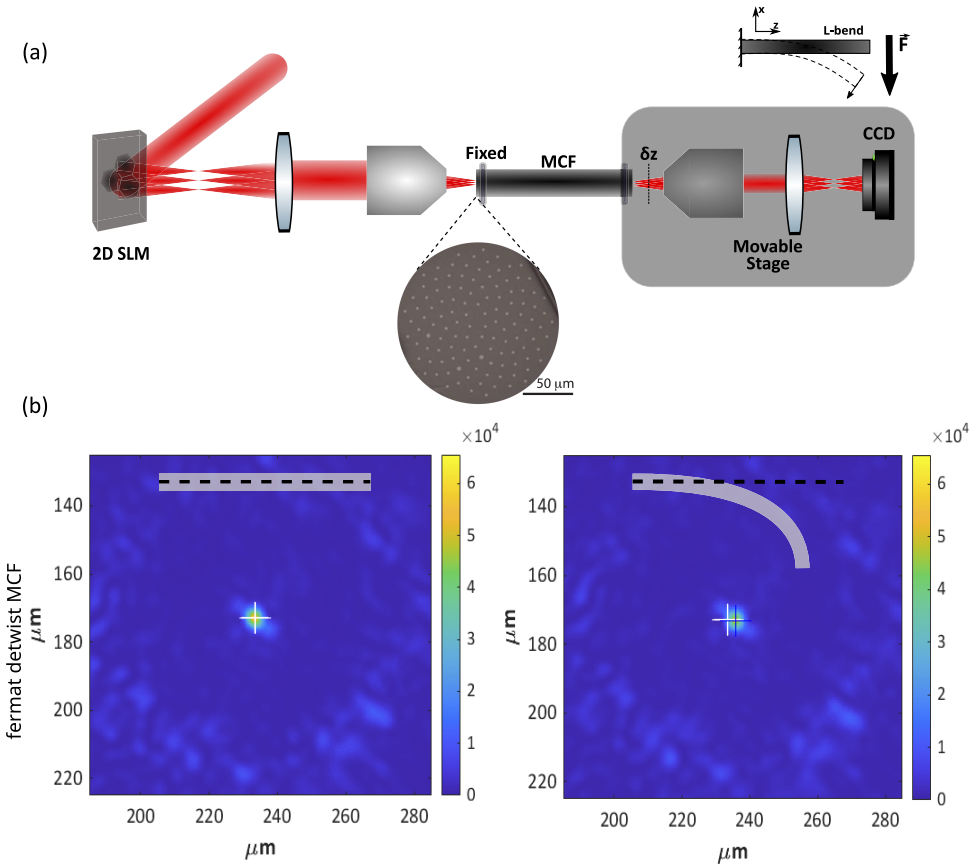

Fig. 4. (a) Setup for bending sensitivity measurements. Inset shows the SEM image of an MCF with a Fermat spiral core distribution. (b) Drift in focal spot position for detwist-MCF with $P = 8$ mm (L bend radius of curvature roughly 90°). The insets show the bending of the fiber for the corresponding focus. The white cross indicates the position of the focal spot when the MCF is straight and the blue cross indicates the new position when the MCF is bent by 90°.

optical axis is used to further minimize any field aberrations. Hence, the different cores of the multicore fiber are addressed by translating the i-th core to coincide with the optical axis. The coupling angle into the core being measured is varied by applying a linearly varying phase ramp across the central SLM segment. A correction on the SLM segment position is done to correct the corresponding shift in the beam position at the core entrance.

For each change in the coupling angle, the output intensity at the MCF distal end is measured using the CCD camera. The optimum coupling angle for a given core is taken as the one for which we measure the maximum intensity at the MCF distal plane. Optimum coupling angles into the cores along diagonals d1, d2, and d3 (as shown in Fig. 3(c)) are measured as a function of the radial distance of the core from the center of the MCF. Fig. 3(b) shows the variation of optimum coupling angle (averaged over the 3 diagonals) w.r.t the radial distance from the central core. In the figure the value $\Delta\Theta$ is the absolute value of the difference between θ_i and θ_0, were $\theta_i = \sqrt{(\theta_x^i)^2 + (\theta_y^i)^2}$ for a given core i and θ_0 is the same as for the central core. It is clear that compared to the radially increasing optimum coupling angles in twisted MCF, for the detwist-MCF, the coupling angles are the same for all the cores. The small changes in the value

Optics EXPRESS

of the coupling angle for different cores are in the same order of magnitude as the measurement error (0.01 *rad*).

The bending insensitivity of the detwist-MCFs was tested using the setup shown in Fig. 4(a). The Fermat MCFs were used for these experiments as the contrast of the main central focus spot is much better for these MCFs [17] making it easier to observe the drift of the focus in the field of view (FOV) versus bending. The sensitivity of the MCFs to L bends is tested (shown in Fig. 4(a)). A L-bend is one where one end (proximal) of the fiber is held static and a transverse force is applied to the other end (distal) in order to create a bend. Individual beamlets are coupled into their respective cores with the help of the 2D-SLM. Their phases are corrected such that the beamlets emitted at the distal end of the MCF are in-phase and coherently combine at plane $\delta z = 500\,\mu$m to form a focus, this plane is then imaged onto the CCD. The MCF is then bent (L bend radius of curvature was roughly 90°) and the corresponding drift in the focal position is monitored by the CCD.

An L-bend elongates the cores along the outer curvature of the bend and compresses the cores along the inner curvature. In the case of a straight MCF, this introduces a phase tilt across the cross-section of the MCF in the direction of the bending axis. Without compensation, this induced phase tilt leads to a corresponding translation in the focal spot (at plane δz) [15]. In practice, it was observed that for a straight MCF, the focal spot drifts beyond the limits of the FOV and disappears even for small bending angles. The Fermat-detwist-MCF (P = 8mm) was observed to have only a very small drift (3 μm) in the focal spot position even for a 90° bend as shown in Fig. 4(b). These results are in agreement with previous bending sensitivity studies on twisted MCFs, detailed in [16]. It is to be noted that in the above experiment, the "detwist" 1 cm sections of the MCF were kept static (by clamping the fiber just above the detwist sections) during the bending experiment as only the twisted section is expected to be insensitive to the bending.

Unlike the twisted MCFs, the detwist-MCFs are shown to have coupling angles into different cores independent of the radial distance of the cores from the MCF center. Here we note that as the coupling behaviour of detwisted MCF matches that of the standard MCF, the model used to simulate the focusing performance of a standard MCF describes that of a detwisted MCF as well. Thus the detwist geometry not only allows for an easier coupling into the proximal end of twisted MCFs, but it is also beneficial at the endoscope distal end as it improves the overlapping of the beamlets coming from each core, therefore increasing the relative power ratio at the focus. Most importantly, it allows us to use twisted fibers in lensless endoscope that are functionalized at their distal end with a 3D-printed hypertelescope [18]. We have shown that this miniature hypertelescope enables to concentrate 35 % of the total distal power into the focus at the imaging plane thus making it suitable for 2PEF imaging. The detwist-MCF is also shown to be insensitive to bending as long as the twist periods are sufficiently small compared to the radius of curvature of bending. However, it is essential to keep the detwist sections as short as possible and static during an experiment, as any bends along these sections can introduce drift of the focal spot in the FOV. By keeping the straight section of the fiber as short as possible and encasing these sections in a metallic casing we hope to keep these sections static during real applications such as 2-photon fluorescence imaging of neurons in freely moving mice.

We note here that a decrease in the fiber transmission efficiency for the detwisted fibers as compared to a standard MCF was also observed. We believe this is due to the non-adiabatic transition of the fiber cores from the straight section to the twisted section. Thus, further modelling and experimentation is needed to find the optimum length over which the MCF transmissions from the straight section to the twisted section without any significant loss in the transmission efficiency of the cores. Another challenge is that in practice the twisting of the straight cores of the MCF and the subsequent detwisting of the ends might result in an incomplete twist period. This results in the transmission matrix of the MCF not being fully independent to the bending of

Optics EXPRESS

the fiber if this incomplete section is part of the fiber bend. We attribute the slight shift in the focal spot observed in Fig. 4(b) to this issue.

3. Conclusion

We have introduced and demonstrated a novel detwist-MCF geometry where a twisted MCF is detwisted over a short distance at its proximal and distal ends and becomes suitable to perform bend-insensitive lensless endoscopy. The retained modification is to detwist short (cm to mm) sections of a twisted MCF at the proximal and distal ends to enable in and out-coupling geometries similar to straight MCF, i.e., constant in/out-coupling angle over the MCF cores. This modification eases the coupling in twisted MCF and makes them compatible with functionalized 3D-printed microstructures, such as hypertelescopes that require straight MCF geometry at the distal endoscope part. Combining detwist-MCF with miniature distal hypertelescope should enable future optimal bend-insensitive lensless endoscopy. Further work is needed to optimize the length of the detwist section in order to have an adiabatic transition of energy from the straight section to the twisted section.

Funding. Agence Nationale de la Recherche (ANR-16-CONV-0001 CENTURI, ANR-19-CE19-0019 MEAP, ANR-20-CE19-0028 NAIMA, ANR-21-ESRE-0002 IDEC, ANR-21-ESRE-0003 CIRCUITPHOTONICS).

Acknowledgments. Parts of this work were developed at IRCICA (USR CNRS 3380, https://ircica.univ-lille.fr/) using FiberTech Lille facilities (https://fibertech.univ-lille.fr/en/). This work was supported by the French Ministry of Higher Education and Research, the "Hauts de France" Regional Council, the European Regional Development fund (ERDF) through the CPER "Photonics for Society".

Disclosures. The authors declare no conflicts of interest.

Data availability. Data that support the findings of this study are available from the corresponding author upon reasonable request.

References

1. F. Helmchen and W. Denk, "Deep tissue two-photon microscopy," Nat. Methods **2**(12), 932–940 (2005).
2. D. Psaltis and C. Moser, "Imaging with multimode fibers," Opt. Photonics News **27**(1), 24–31 (2016).
3. E. R. Andresen, S. Sivankutty, V. Tsvirkun, G. Bouwmans, and H. Rigneault, "Ultrathin endoscopes based on multicore fibers and adaptive optics: a status review and perspectives," J. Biomed. Opt. **21**(12), 121506 (2016).
4. T. Čižmár and K. Dholakia, "Shaping the light transmission through a multimode optical fibre: complex transformation analysis and applications in biophotonics," Opt. Express **19**(20), 18871 (2011).
5. E. R. Andresen, G. Bouwmans, S. Monneret, and H. Rigneault, "Two-photon lensless endoscope," Opt. Express **21**(18), 20713–20721 (2013).
6. E. E. Morales-Delgado, D. Psaltis, and C. Moser, "Two-photon imaging through a multimode fiber," Opt. Express **23**(25), 32158 (2015).
7. S. Sivankutty, E. R. Andresen, R. Cossart, G. Bouwmans, S. Monneret, and H. Rigneault, "Ultra-thin rigid endoscope: two-photon imaging through a graded-index multi-mode fiber," Opt. Express **24**(2), 825 (2016).
8. A. J. Thompson, C. Paterson, M. A. A. Neil, C. Dunsby, and P. M. W. French, "Adaptive phase compensation for ultracompact laser scanning endomicroscopy," Opt. Lett. **36**(9), 1707 (2011).
9. E. R. Andresen, G. Bouwmans, S. Monneret, and H. Rigneault, "Toward endoscopes with no distal optics: video-rate scanning microscopy through a fiber bundle," Opt. Lett. **38**(5), 609 (2013).
10. M. Kim, W. Choi, Y. Choi, C. Yoon, and W. Choi, "Transmission matrix of a scattering medium and its applications in biophotonics," Opt. Express **23**(10), 12648–12668 (2015).
11. J. C. Roper, S. Yerolatsitis, T. A. Birks, B. J. Mangan, C. Dunsby, P. M. W. French, and J. C. Knight, "Minimizing group index variations in a multicore endoscope fiber," IEEE Photonics Technol. Lett. **27**(22), 2359–2362 (2015).
12. S. Sivankutty, V. Tsvirkun, G. Bouwmans, D. Kogan, D. Oron, E. R. Andresen, and H. Rigneault, "Extended field-of-view in a lensless endoscope using an aperiodic multicore fiber," Opt. Lett. **41**(15), 3531–3534 (2016).
13. S. Ohayon, A. Caravaca-Aguirre, R. Piestun, and J. J. DiCarlo, "Minimally invasive multimode optical fiber microendoscope for deep brain fluorescence imaging," Biomed. Opt. Express **9**(4), 1492 (2018).
14. S. A. Vasquez-Lopez, R. Turcotte, V. Koren, M. Plöschner, Z. Padamsey, M. J. Booth, T. Čižmár, and N. J. Emptage, "Subcellular spatial resolution achieved for deep-brain imaging in vivo using a minimally invasive multimode fiber," Light: Sci. Appl. **7**(1), 110 (2018).
15. V. Tsvirkun, S. Sivankutty, G. Bouwmans, O. Vanvincq, E. R. Andresen, and H. Rigneault, "Bending-induced inter-core group delays in multicore fibers," Opt. Express **25**(25), 31863–31875 (2017).
16. V. Tsvirkun, S. Sivankutty, K. Baudelle, R. Habert, G. Bouwmans, O. Vanvincq, E. R. Andresen, and H. Rigneault, "Flexible lensless endoscope with a conformationally invariant multi-core fiber," Optica **6**(9), 1185–1189 (2019).

Optics EXPRESS

17. S. Sivankutty, V. Tsvirkun, O. Vanvincq, G. Bouwmans, E. R. Andresen, and H. Rigneault, "Nonlinear imaging through a fermat golden spiral multicore fiber," Opt. Lett. **43**(15), 3638–3641 (2018).
18. S. Sivankutty, A. Bertoncini, V. Tsvirkun, N. G. Kumar, G. Brévalle, G. Bouwmans, E. R. Andresen, C. Liberale, and H. Rigneault, "Miniature 120-beam coherent combiner with 3d-printed optics for multicore fiber-based endoscopy," Opt. Lett. **46**(19), 4968–4971 (2021).